ISSN: 2594 - 2905

# CHARACTERIZATION OF A PILOT BMS SYSTEM BASED ON LI-ION BATTERIES FOR ELECTRIC VEHICLE APPLICATIONS

# CHARACTERIZATION OF A PILOT BMS SYSTEM BASED ON LITHIUM-ION BATTERIES FOR ELECTRIC VEHICLE APPLICATIONS

Guevara-Ramírez Álvaro César[1] , Jarquín-Flores Héctor Javier[2] , Cruz-Valdiviezo Alfredo[3] , Silva-Cruz Eric Mario[4] , Lastre Domínguez Carlos Mauricio[5]

https://doi.org/10.61117/ipsumtec.v9i1.445

[1] National Technological Institute of Mexico/Oaxaca Technological Institute, Department of Electrical and Electronic Engineering.alvaro.guevara@itoaxaca.edu.mx , 0009-0008-1279-6911
[2] National Technological Institute of Mexico/Oaxaca Technological Institute, Department of Electrical and Electronic Engineering.hector.jarquin@itoaxaca.edu.mx , 0009-0004-7342-838X
[3] National Technological Institute of Mexico/Oaxaca Technological Institute, Department of Electrical and Electronic Engineering.alfredo.cruz@itoaxaca.edu.mx , 0009-0002-3489-5116
[4] National Technological Institute of Mexico/Oaxaca Technological Institute, Department of Electrical and Electronic Engineering.eric.cruz@itoaxaca.edu.mx , 0000-0002-0496-9682
[5] National Technological Institute of Mexico/Oaxaca Technological Institute, Department of Electrical and Electronic Engineering.carlos.lastre@itoaxaca.edu.mx , 0000-0003-2737-7644

***Abstract*** -- A methodology for an open battery management system (BMS) using LiFePO4 batteries in electric vehicles is presented. In the experimental phase, a 12 V–15 Ah module is implemented with Raspberry Pi Pico and INA219, calibrated with a multimeter and recorded in CSV/SQLite, calculating energy by real Δt. The State of Charge (SOC) is estimated using a hybrid approach that combines the OCV–SOC curve for LFP and Coulomb counting with a filter, useful in the flat region. A simulation environment is developed for a 48 V–20 Ah (16S) pack with a Thévenin model to evaluate performance in different cycles and compare KPIs: energy, I2R losses, minimum voltage, and SOC error, with respect to a test bench. In bench tests, with a 10Ω (~15 W) load, ohmic consistency and stability of less than 2% were observed. The simulation showed SOC errors of 1.6–2.4% (MAE) and 2.4–3.1% (RMSE), with
adequate voltage margins. The proposed architecture is reproducible, portable for SBC, and scalable to a 16S pack with adequate sensing and isolation.

***Keywords***: Battery Management System, INA219, LiFePO4, Thévenin model, Raspberry Pi Pico, SOC.

***Abstract*** -- An open BMS for LiFePO4 batteries in EVs is presented. An experimental setup uses a 12 V–15 Ah module with Raspberry Pi Pico and INA219, calibrated against a multimeter, recording data in CSV/SQLite and calculating energy via real Δt. A hybrid SOC estimation combines OCV–SOC curve and Coulomb counting with a filter, effective in flat regions. A simulation for a 48 V–20 Ah pack with a Thévenin model assesses performance across different cycles, comparing energy, I2R losses, voltage, and SOC error against a test bench. Bench tests with a 10Ω load showed less than 2% stability. Simulations yielded SOC errors of 1.6–2.4% (MAE) and
2.4–3.1% (RMSE). The architecture is reproducible, portable to SBC, and scalable to 16S packs with appropriate sensing and isolation.

***Key words –*** Battery Management System, INA219, LiFePO4, Raspberry Pi Pico, SOC, Thevenin model.

## INTRODUCTION

A Battery Management System (BMS) is responsible for preserving the operational safety of the electrochemical system, monitoring critical variables (voltage, current, temperature), estimating latent states such as State of Charge (SOC) and State of Health (SOH), and applying protection and balancing strategies that extend the autonomy and useful life of the battery pack [1][2][3][4]. In vehicle applications, these functions must be performed with low latency and high data traceability [5][6][7]. Among Li-ion chemistries, LiFePO4 (LFP) stands out for its thermal stability and safe operating window [8][9][10][11]. [12] provides a review of key technologies and future trends essential for addressing sustainability in electric vehicles.
However, its OCV–SOC relationship has a relatively flat central section that limits observability.

of the state based on the measured voltage, especially under load. Consequently, exclusively voltammetric methods are insufficient and must be complemented with current integration (coulomb counting) and re-anchoring mechanisms during rest or after full charges [13][14][15][16]. Additionally, hysteresis effects, dependence on the charge/discharge rate, and thermal interaction introduce biases if not explicitly modeled [17][18][19]. This article presents an integrated methodology for the design, instrumentation, and validation of a BMS oriented to electric vehicles with LFP, covering: (i) a
(i) inexpensive and reproducible experimental instrumentation at 12~V with I2C acquisition and traceable recording; (ii) an estimation chain based on a hybrid SOC that
merges coulomb counting with OCV-SOC anchors using a complementary filter; and (iii) a digital bank with a Thévenin model of a pole for a 48~V--20~Ah (16S) pack, with evaluation in cycles for urban, extra-urban, and mixed scenarios with their respective regeneration. The common thread is the physical-electrical consistency of the measurements, the
data flow reproducibility, and compatibility with embedded hardware execution. The main contributions of this work are as follows:

- Hybrid Precision SOC Estimator: Development of a hybrid Coulomb + OCV algorithm for LFP batteries with low MAE error approx. 1.6–2.4.
- Simulation of a 48 V pack using a Thévenin model in one pole to simulate a 48 V-20 Ah pack in real driving cycles.
- Implementation of a small-scale BMS system.

## DEVELOPMENT

### Materials

For this research, a 12 V, 15 Ah LFP battery, an INA219 device [20] with a 0.1 Ω shunt resistor, a 10 Ω load resistor of
15 W, 20×4 LCD display via PCF8574 [21], and I²C bus.

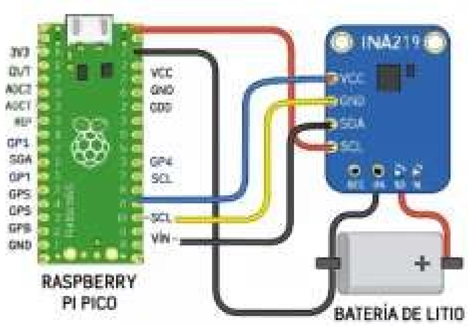


**Figure 1**: *Schematic diagram of the BMS*

**Source**: *Own elaboration.*

The main microcontroller is the Raspberry PI PICO.
[22] based on the RP2040 chip [23]. Figure 1 shows a general diagram of the hardware used to carry out this research project. In terms of software, we worked with the MicroPython platform.

### Mathematical model for SOC estimation

For the hybrid SOC estimation, we based ourselves on the general coulombimetry model defined in works [24] and [25]. This model is defined by equation (1),

$$SOC(t) = SOC(t_{(0)}) - \frac{100}{C_{nom}} \int_{t_o}^{t} I(\tau)\, d\tau \qquad \text{Eq. (1)}$$

Where $C_{nom}$ is the effective capacity measured in ampere-hours (Ah), $SOC(t_0)$ is the initial state of charge, and the current $I(\tau)$ is the instantaneous positive current during discharge. For discrete implementation under the time step Δt, equation (2) is considered.
equation (2),

$$\hat{s}_k^{coul} = \hat{s}_{k-1} - \frac{100 I_k \Delta t}{C_{nom}(3600)} \qquad \text{Eq. (2)}$$

Where $\hat{s}_k^{coul}$ is the SOC estimated by coulombimetry at discrete instant k and $I_k$ is the measured current (positive during discharge), $\hat{s}_k$ corresponds to the hybrid estimated SOC, obtained from the fusion between the coulombimetric estimator and the voltimetric anchor, The index $k$ denotes the discrete time instant and Δt the integration step in seconds.
For voltmetric anchoring, an OCV-SOC table described in [26] is used, where each LFP cell is analyzed by linearly interpolating to obtain $\hat{s}_k^{ocv}$ from
from the *pack* voltage $V_k$ with $N$ cells in series
$v_{celda} = V_k / N$. This average voltage value per cell is associated with the corresponding point on the OCV–SOC curve
SOC curve, thus allowing equation (2) to be related to the voltimetric behavior. Therefore, the discrete state of charge is defined by equation (3)

$$\hat{s}_k = \alpha_k \hat{s}_k^{coul} + (1-\alpha_k)\hat{s}_k^{ocv} \qquad \text{Eq. (3)}$$

where $\hat{s}_k \in [0,100]$ and $\alpha_k \in [0,1]$, which weights greater weight to Coulomb under load-regeneration and greater weight to OCV at rest. It is recharged during prolonged rest if the following expression described by equation (4) is satisfied:

$$|I_k| < I_{rest}, \left|\frac{\Delta V}{\Delta t}\right| < \varepsilon_v \qquad \text{Eq. (4)}$$

Where $I_{rest}$ represents the maximum current threshold for considering rest (typically less than 0.1A), $\varepsilon_v$ is the allowed temporary voltage variation limit (by example, 1mV/s), $\left|\frac{\Delta V}{\Delta t}\right|$ corresponds to the voltage gradient

$T_{rest}$ measured in the observation window, this evaluation is carried out during the time interval defined as the time

minimum consecutive time during which the battery remains without active charging or discharging. During this period, the system current is practically zero and the voltage terminal tends to stabilize, allowing us to consider that the battery has reached its electrical rest state. To suppress the pulses provided in equations (2) and (3), a moving average filter with windows of five and 10 samples for the voltage variables $V$ and current $I$.

**Mathematical model for battery**

In this work, an equivalent model of Thévenin of a pole with $R_0$ in series and a filter consisting of $R_1$ and $C_1$ at the pakk 16S level, [26]. The terminal voltage is determined by equations (5) and (6),

$$V_k = (N).(OCV).(S_k) - I_k R_0 - V_{RC,k} \qquad \text{Eq. (5)}$$

Where,

$$V_{RC,k} = V_{RC,k-1} + \Delta t\left(\frac{V_{RC,k-1}}{R_1 C_1} + \frac{I_k}{C_1}\right) \qquad \text{Eq. (6)}$$

The base parameters are summarized in Table 1, where a time $\tau = R_1 C_1$ is used, which includes the transient relationship. This model generates the traces of the voltage variables $V$, current $I$ and power $P$.

**Table 1**. *Reference and actual measurements of the system.*

| Magnitude | Value | Unit |
|---|---|---|
| Capacity $Q_{nom}$ | 20 | Ah |
| Cells in series $N$ | 16 | -- |
| $R$series resistance $_0$ | 0.050 | Ω |
| RC branch: $R_1$ and $C_1$ | 0.020<br>100 | Ω<br>F |
| Time constant $\tau R_1 C_1$ | 20 | $s$ |
| Integration step $\Delta t$ | 1 | $s$ |
| Complementary weight $\alpha$ | 0.85 | -- |

**Source**: *Own elaboration*.

**Driving scenarios and performance metrics**

In this context, three driving scenarios or cycles are considered: urban, extra-urban, and mixed, which is a combination of both. Under certain conditions of current $I_k$ and time $\Delta t$, the net energy $E_{net}$ of the system is calculated in KPIs using the equation (7),

$$E_{net} = \sum_{k=1}^{K} \frac{V_k I_k \Delta t}{3600} \qquad \text{Ec. (7)}$$

Losses are calculated from equation (8),

$$Pérdida = \sum_{k=1}^{K} \frac{I_k^2 R_{(0)} \Delta t}{3600} \qquad \text{Ec. (8)}$$

Finally, the MAE and RMSE errors for the SOC $\hat{S}$ estimation$_k$, both for the real $\hat{S}_k$, consider equations (9) and (10)

$$MAE_{SOC} = \frac{1}{K}\sum_{k=1}^{K} |\hat{S}_k - S_k|, \qquad \text{Ec. (9)}$$

$$RMSE_{SOC} = \sqrt{\frac{1}{K}\sum_{k=1}^{K}(\hat{S}_k - S_k)^2} \qquad \text{Eq. (10)}$$

**Pseudocodes for SOC simulation**

The three pseudocodes describe a simulation algorithm for a Battery Management System (BMS) centered on an LFP package. Algorithm 1 manages the initialization of the data, defining the structure of the package (Thévenin model parameters:

$R\_0$, $R\_1$, $C\_1$ and establishing the OCV_de_SOC function, which uses linear interpolation on a reference table to obtain the open-circuit cell voltage.

**Algorithm 1: Data Structures and OCV-SOC**

1. **Require:** OCV_TABLE curve
2. **Ensure:** Defined LiFePO4 package structure and OCV_de_SOC function available
3. **LiFePO4 Package Structure**
4. { Q_Ah, N_series
5. **R0, R1, C1;**
6. Q_Ah_actual, SOC_pc, V_rc; }
7. **FunctionOCV_de_SOC(**SOC_pc, OCV_table**):**
8. **if** SOC_pc is in OCV_TABLE **then**
9. **Return** V_OCV
10. **else**
11 **Return** **linear_interpolation**(OCV_TABLE, SOC_pc)
**end if**
5. **End Function**

Algorithm 2 contains the core of the SIMULAR_PASO simulation, which, for each $\Delta t$, updates the polarization voltage $V_{rc}$ by integrating the Thévenin model, calculates the terminal voltage, and estimates the State of Charge (SOC) using the Coulomb count from the current. Finally, Algorithm 3 is responsible for executing the cycle, iterating the function

SIMULATE_STEP along a predefined current profile, and accumulating key performance metrics (KPIs), such as net energy, losses $I^2R$, and voltage limits, to generate the complete log of the simulation

**Algorithm 2 Discrete-time integration**

1. **Require:** dt, I, Pack
2. **Ensure:** Pack, V_term
3. **Function SIMULATE_STEP(**dt, I, Pack**):**
4. V_ocv_pack ← Pack.N_series × OCV_of_SOC(Pack.SOC_pc)
5. dV_rc ← ((I / Pack.C1) - (Pack.V_rc / (Pack.R1 × Pack.C1))) × dt
6. Pack.V_rc ← Pack.V_rc + dV_rc
7. V_terminal ← V_ocv_pack - Pack.V_rc - (Current_I × Pack.R0)
8. Pack.Q_Ah_current ← Pack.Q_Ah_current - (Current_I × dt / 3600)
9. Pack.SOC_pc ← (Pack.Q_Ah_actual / Pack.Q_Ah) × 100
10. **Return** V_terminal
11. **End Function**

**Algorithm 3 cycle execution and recording**

1. **Require:** Pack, PCT, dt.
2. **Ensure:** Log_Dat, KPI
3. **Function execute_cycle(**Pack,PCT, dt**):**
4. Log_Dat ← empty_list
5. **Initialize(**Ener, Perdi, V_min, V_max**)**
6. **for** each (I_com, Dur) **in** PCT**:**
7. Time ← 0
8. **while** Current_time < Duration **do**
9. **V_actual←simulate_step(**dt, I_com, Pack**)**
10. Power_W ← V_actual × I_command
11. Ener ← Ener + (Power × dt / 3600)
12. Per ← Per + ((I_com² × Pack.R0) × dt / 3600
13. V_min ← **min(**V_min, V_act**)**
14. V_max ← **max(**V_max, V_act
15. **Add to Data_Log: (**Time, V_act, I_command, Energy, Pack
16. Time ← Time + dt
17. **end while**
18. **end for**
19. **KPIs** ← **{**Ener, Per, V_min, V_max, Pack.SOC_pc}
20. **Return** Log_Data, KPI
21. **End Function**

## DISCUSSION AND ANALYSIS OF RESULTS

### Calibration and acquisition of the BMS

As shown in Figure 2, the test bench used for characterization at 12 V is shown, with the high-current loop routed through the INA219 shunt and the I²C interface, together with the LCD display. The typical ranges of voltage, current, power, and SOC obtained under the 10 Ω resistive load are described in Table 2. Regarding traceability, a comparative table of actual values, simulated values, and relative error, averaging the actual readings (see Table 3). Table 4 summarizes the uncertainty budget. These are associated with load tolerances of 5%, voltage drop in cables and/or connectors, current offset in the INA219, ADC quantization noise, and jitter effect in sampling. With a nominal load of 10 Ω and a voltage of approximately 12.8, Table 5 summarizes the averages.
standard deviations and fluctuation (p95) of electrical variables describing the temporal stability of the time step Δt, voltage$V$, current$I$ , and finally the power $P$.

**Table 2**. *Typical averaged measurements involved*

| Magnitude | Range | Source |
|---|---|---|
| Voltage (V) | 12.7-12.9 | INA219 |
| Current (A) | 1.18-1.32 | INA219 |
| Power (W) | 14.7-17.0 | V × I |
| SOC (%) | 88-92 | Hybrid (OCV + Coulomb) |

**Source**: *Own elaboration*.

**Table 3**. *Reference and actual measurements of the system.*

| Magnitude | Reference | INA219 (Actual) | Relative error (%) |
|---|---|---|---|
| Voltage (V) | 12.82 | 12.64 | 1.4 |
| Current (A) | 1.28 | 1.25 | 2.3 |
| Power (W) | 16.4 | 15.8 | 3.7 |

**Source**: *Prepared internally*.

**Table 4**. *Uncertainty budget.*

| Metric | Typical contribution |
|---|---|
| Load tolerance (5%) | 0.5–0.8W |
| Voltage drops in cables/connectors | 10–40 mV |
| INA219 current offset | 2–8 mA |
| ADC quantization noise | ± 1 LSB (voltage/current) |
| Sampling jitter | <10 ms (P95) |

**Source**: Own elaboration.

**Table 5**. *Statistics on the temporal stability of the variables.*

| Magnitude | Average $\mu$ | Standard deviation $\sigma$ | p95 |
|---|---|---|---|
| Time step Δt (s) | 0.99 | 0.03 | 1.05 |
| $V$ e voltage (V) | 12.80 | 0.06 | 12.91 |
| $I$ e current (A) | 1.26 | 0.03 | 1.31 |
| $P$ d power (W) | 15.95 | 0.32 | 16.54 |

**Source**: *Own elaboration*.

### Variable recording and ohmic consistency

As can be seen in Figure 3, the implementation of the circuit yields data that is sampled at a frequency of 1 Hz and shows the stability of the voltage and current variables with a variation of less than 2% in a 60-second interval. In addition, ohmic consistency can be verified with the nominal load of 10 Ω and the
different variables involved, such as voltage, current, power, and SOC percentage. This was verified using Ohm's law. Additionally, the accumulated energy can be calculated indirectly based on the real time associated with the time interval Δt.

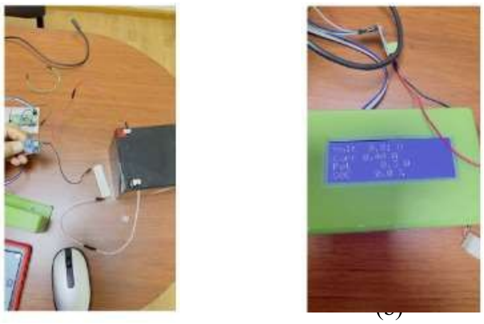

**Figure 2**. *Experimental development. (a) Test bench with the LFP 12 V module and INA219. (b) Measurements of electrical variables sampled at 1 kHz.*
**Source**: *Own work*.

**Development of simulations for urban, extra-urban, and mixed scenarios.**
Based on equations (1) to (6), simulations are developed in three scenarios: urban, extra-urban, and mixed. Summary of duration, maximum current$I_{max}$,
average current $\bar{I}$, and fraction of energy generated is
is presented in Table (6).

**Table 6**. *Description of duration in seconds, maximum current, average current, and energy generation*

| Scenario | Dur. (s) | $I_{max}$ (A) | $\bar{I}$ $(A)$ | Rainfall (%) |
|---|---|---|---|---|
| Urban | 200 | 30 | 12.5 | 12 |
| Extra-urban | 370 | 35 | 18.0 | 10 |
| Mixed | 300 | 32 | 14.0 | 15 |

**Source**: *Own elaboration*.

As can be seen in Table 7, the different KPIs are described in cycles for the scenarios mentioned.

**Table 7**. *KPIs in cycles. Urban, extra-urban, and mixed*

| Scenario | $E_{net}$ (Wh) | $V_{min}$ (V) | $P_e$ (Wh) | $SOC_f$ ( |
|---|---|---|---|---|
| Urban | **80** | 45 | 8 | 93 |
| Extra-urban | 140 | 44 | 12 | 89 |
| Mixed | 110 | 44.6 | 9.6 | 91 |

**Source**: *Own elaboration*.

Figures (3), (4), and (5) show the different SOC behaviors based on a comparison between the true SOC and the estimated SOC for the different urban, extra-urban, and mixed scenarios.

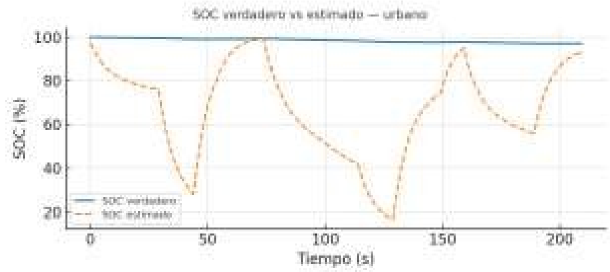


**Figure 3**. *True SOC vs. estimated SOC in an urban scenario.*
**Source**: *Own elaboration*.

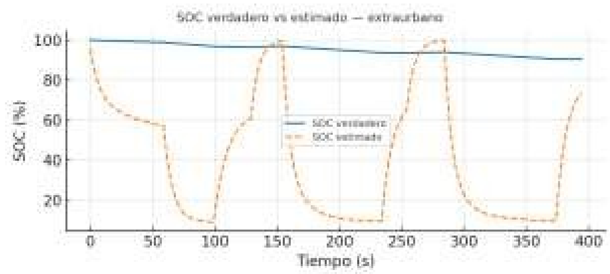


**Figure 4**. *True SOC vs. estimated SOC in extra-urban setting.*
**Source**: Author's *own work*.

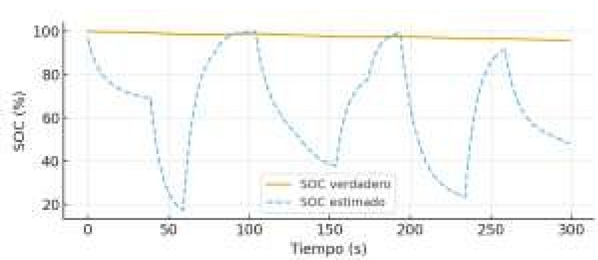


**Figure 5**. *True SOC vs. estimated SOC in mixed scenario.*
**Source**: *Own elaboration*.

The voltage and current trajectories are shown in Figures (6), (7), and (8), while the instantaneous power and energy are shown in Figures (9), (10), and (11). Table 7 shows the aggregate KPIs associated with net energy, minimum voltage, losses, final SOC, and stored energy.

ISSN: 2594 - 2905

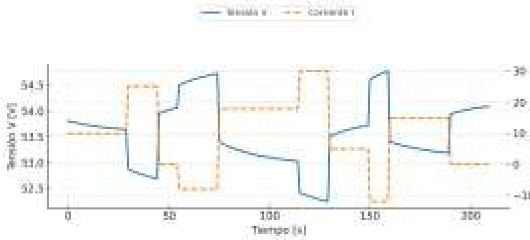

**Figure 6**. *Urban scenario: voltage (solid line) and current (dashed line).*

**Source**: *Own elaboration*.

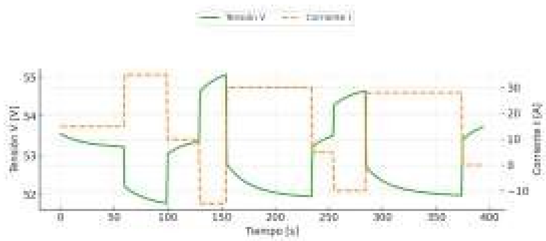

**Figure 7**. *Extra-urban scenario: voltage (solid line) and current (dotted line).*

**Source**: *Own elaboration*.

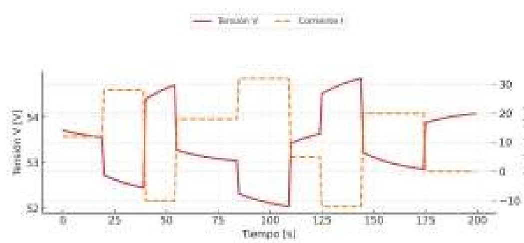

**Figure 8**. *Mixed scenario: voltage (solid line) and current (dotted line).*

**Source**: *Own elaboration*.

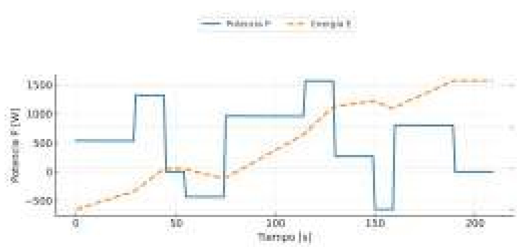

**Figure 9**. *Urban scenario: power (solid line) and energy (dotted line).*

**Source**: *Own elaboration*.

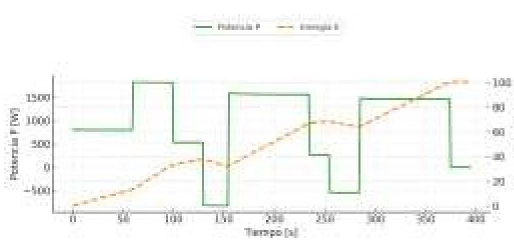

**Figure 10**. *Extra-urban scenario: Power (solid line) and energy (dotted line).*

**Source**: *Own elaboration*.

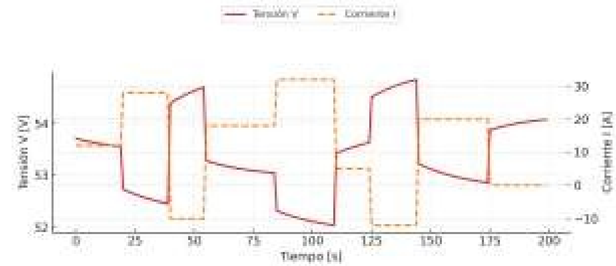

**Figure 11**. *Mixed scenario: power (solid line) and energy (dotted line).*

**Source**: Author's *own work*.

**Model performance analysis and voltage margins and losses**

Once the simulation had been carried out in the urban, extra-urban, and mixed scenarios, the model performance was analyzed using the root mean square error (RMSE), mean absolute error (MAE), relative error ($E_{re}$ ), and open-circuit voltage (OCV)
($OCV_a$) for re-anchors or SOC correction points.
In Table (8), we can observe the performance indices performance indices for the different scenarios.

**Table 8**. *Performance of the error of the model associated with SOC and energy.*

| Scenario | MAE (%) | RMSE | $OCV_a$ | $E_{re}$ (%) |
|---|---|---|---|---|
| Urban | 1.6 | 2.4 | 3 | 1.3 |
| Extra-urban | 2.4 | 3.1 | 2 | 1.9 |
| Mixed | 1.9 | 2.7 | 3 | 1.5 |

**Source**: Own elaboration.

Given the calculation of errors, the different margins and losses associated with SOC were analyzed. For the *under-voltage* (UV) threshold of 42 V at a pack level of 2,625 V/cell, the resulting margins and losses are described in Table 9. Here we observe that the$V_{min}$
the extra-urban scenario is the lowest, presenting a lower margin at UV. The urban cycle has lower losses due to lower average currents.

**Table 9**. *Minimum voltage margin to UV and losses with UV threshold 42 [V].*

| Scenario | MAE (%) | RMSE | $OCV_a$ | $E_{re}$ (%) |
|---|---|---|---|---|
| Urban | 1.6 | 2.4 | 3 | 1.3 |
| Extra-urban | 2.4 | 3.1 | 2 | 1.9 |
| Mixed | 1.9 | 2.7 | 3 | 1.5 |

**Source**: *Own elaboration*.

The single pole associated with Thévenin adequately represents short- and medium-term dynamics at a low computational cost, which is sufficient for line estimation. Accuracy depends on the OCV per cell and the identification of $R_0$ ,$R_1$ and ,$C_1$ . Regarding the robustness of the model, the Coulomb+OCV combination reduces the flat region (LFP) and the drift-integrator. This allows the SOC to be re-anchored during rest phases or after full charges. The errors observed are compatible with monitoring requirements in vehicle prototypes. In terms of experimental development and scalability, greater margin sensing is required in isolated common mode due to the Hall effect. A protected divider for bus voltage, coordinated fuses together with the contactor, and precharge are also necessary. Other options could be considered, such as the Raspberry Pi 5 [33], which could enable adequate persistent logging and leverage *dashboarding* systems such as *Grafana-flash* or *Node-Red*. Finally, the limitations of this research development are associated with simulation. This development does not include essential parameters such as thermal gradients and degradation.

## CONCLUSIONS

Modeling and simulation were applied to an open battery management system with LiFePO4 chemistry, ensuring traceability from a 12 V bank to a 48 V–20 Ah (16S) pack. A reliable acquisition chain was established with time control, ohmic consistency, and stability of less than 2%, in addition to multimeter calibrations. The software calculated power and energy to estimate the State of Charge (SOC). Simulation with the Thévenin model and coulombimetry and OCV–SOC techniques showed errors in SOC of 1.6–2.4% (MAE) and 2.4–3.1% (RMSE).

Re-anchoring at rest stabilized the drift. KPIs, such as $E_{net}$ and $V_{min}$ , confirmed adequate margins for tension. The architecture is compatible with low-power platforms, such as Raspberry Pi 5, and is scalable to hybrid vehicles. Overall, the results support the use of a hybrid estimator, due to its low computational cost and support in the technical literature.

As future work, more iterations and more robust thermal models, such as *lumped* models and validation with *drive cycles*, will be considered.

## ACKNOWLEDGMENTS

We would like to thank the facilities of the National Technological Institute of Mexico, Oaxaca Technological Institute, which endorsed the project with code 2355.25-P.

## BIBLIOGRAPHY

[1] National Renewable Energy Laboratory (NREL), "Battery Management Systems (BMS) Overview," 2024. Available at: https://www.nrel.gov/ transportation/battery-management-systems.html

[2] M. A. Hannan, M. S. H. Lipu, A. Hussain, and A. Mohamed, "A review of lithium-ion battery state of charge estimation and management system in electric vehicle applications," Renewable and Sustainable Energy Reviews, vol. 78, pp. 834–854, 2017.

[3] Krishna, T. N. V., et al. "Powering the future: Advanced battery management systems (BMS) for electric vehicles." *Energies* 17.14 (2024): 3360.

[4] Pattnaik, Manasi, Manoj Badoni, and H. P. Singh. "Analysis of electric vehicle battery system." *2021 4th International Conference on Recent Developments in Control, Automation & Power Engineering (RDCAPE)*. IEEE, 2021.

[5] Thangavel, Saravanakumar, et al. "A comprehensive review on electric vehicles: battery management systems, charging stations, traction motors." *IEEE access* 11 (2023): 20994-21019.

[6] Ramkumar, M. Siva, et al. "Review on Li-Ion Battery with Battery Management System in Electrical Vehicle." *Advances in Materials Science and Engineering* 2022.1 (2022): 3379574.

[7] Challoob, Ali Falih, et al. "Energy and battery management systems for electric vehicles: A comprehensive review & recommendations." *Energy Exploration & Exploitation* 42.1 (2024): 341-372.

[8] Habib, AKM Ahasan, et al. "Lithium-ion battery management system for electric vehicles: constraints, challenges, and recommendations." *Batteries* 9.3 (2023): 152.

[9] Guo, Jian, and Fangming Jiang. "A novel electric vehicle thermal management system based on cooling and heating of batteries by refrigerant." *Energy Conversion and Management* 237 (2021): 114145.

[10] Komsiyska, Lidiya, et al. "Critical review of intelligent battery systems: Challenges, implementation, and potential for electric vehicles." *Energies* 14.18 (2021): 5989.

[11] Lipu, Molla Shahadat Hossain, et al. "Battery management, key technologies, methods, issues, and future trends of electric vehicles: A pathway toward achieving sustainable development goals." *Batteries* 8.9 (2022): 119.

[12] Ali, Muhammad Umair, et al. "Towards a smarter battery management system for electric vehicle applications: A critical review of lithium-ion battery state of charge estimation." *Energies* 12.3 (2019): 446.

[13] Ali, Muhammad Umair, et al. "Towards a smarter battery management system for electric vehicle applications: A critical review of lithium-ion battery state of charge estimation." *Energies* 12.3 (2019): 446.

[14] Lin, Qian, et al. "Towards a smarter battery management system: A critical review on optimal charging methods of lithium ion batteries." *Energy* 183 (2019): 220-234.

[15] Hossain Lipu, Molla Shahadat, et al. "Smart battery management technology in electric vehicle applications: Analytical and technical assessment toward emerging future directions." *Batteries* 8.11 (2022): 219.

[16] Xiong, Rui, Linlin Li, and Jinpeng Tian. "Towards a smarter battery management system: A critical review on battery state of health monitoring methods." *Journal of Power Sources* 405 (2018): 18-29.

[17] X. Hu, S. Li, and H. Peng, "A comparative study of equivalent circuit models for Li-ion batteries," Journal of Power Sources, vol. 198, pp. 359–367, 2012.

[18] H. He, R. Xiong, and H. Guo, "Online estimation of model parameters and state-of-charge of LiFePO4 batteries," Applied Energy, vol. 89, pp. 413–420, 2012.

[19] G. L. Plett, "Extended Kalman filtering for battery management systems of LiPB-based HEV battery packsPart 1: Background," Journalof Power Sources, vol. 134, no. 2, pp. 252–261, 2004.

[20] O. Tremblay and L.-A. Dessaint, "Experimental validation of a battery dynamic model for EV applications," in Proc. IEEE VPPC, 2009, pp. 1–5.

[21] Texas Instruments, "INA219: Zero-Drift, Bidirectional Current/Power Monitor With I2C Interface," Datasheet. Available at: https://www.ti.com/product/INA219

[22] Raspberry Pi Ltd., "RP2040 Datasheet," 2024. Available at: https://datasheets.raspberrypi.com/rp2040/rp2040-datasheet.pdf

[23] Raspberry Pi Ltd., "Raspberry Pi Pico Datasheet," 2024. Available at:https://datasheets.raspberrypi.com/pico/pico-datasheet.pdf

[24] NXP Semiconductors, "PCF8574/PCF8574A Remote 8-bit I/O expander for I2C-bus," Datasheet. Available at: https://www.nxp.com/docs/en/data-sheet/PCF8574_PCF8574A.pdf

[25] Raspberry Pi Ltd., "Raspberry Pi 5 Product Brief," 2023. Available at:https://www.raspberrypi.com/products/raspberry-pi-5/

[26] Texas Instruments, "INA219: Zero-Drift, Bidirectional Current/Power Monitor With I2C Interface," Datasheet. Available at: https://www.ti.com/product/INA219


**Contribution Role Table**

| Role | Author(s) |
|---|---|
| Administration Project, Validation, and Resources | Álvaro César Guevara Ramírez |
| Supervision, Software, Methodology, Writing, and Validation | Hector Javier Jarquín Florés |
| Conceptualization and Writing | Alfredo Cruz Valdiviezo |
| Conceptualization and Visualization | Eric Mario Silva Cruz |
| Administration Project, Validation Supervision, Software and Writing | Carlos Mauricio Lastre Domínguez |